Seasonal influenza viruses show distinct adaptive dynamics during growth in chicken eggs

Kathryn Kistler[1,2][*], Trevor Bedford[1,2]

[1] Vaccine and Infectious Disease Division, Fred Hutchinson Cancer Center, Seattle, WA, USA

[2] Howard Hughes Medical Institute, Seattle, WA, USA

* corresponding author

Abstract

Human influenza viruses are grown in chicken eggs for vaccine production. Sequences of these egg-passaged viruses give us the opportunity to examine the evolution that occurs when these human viruses are subjected to the selective pressure of growing in chicken eggs, which (among other things) express different sialic acid receptors. The repetition of this evolutionary experiment in hundreds of strains over the past several decades allows us to identify mutations that adapt the virus to eggs and epistatic constraints that influence them. We analyze influenza A/H3N2, A/H1N1pdm, B/Vic and B/Yam sequences that were passaged in eggs and find that almost all of the adaptive mutations are located around the receptor-binding pocket of hemagglutinin (HA). We observe epistatic interactions both between adaptive mutations and between these mutations and the continually-evolving human influenza HA background sequence. Our results show that this background dependence is greatest for influenza A/H3N2, then A/H1N1pdm, with B/Vic and B/Yam showing little-to-no background dependence. We find that the total number of adaptive mutations and the length of adaptive walk also follow the same pattern between the influenza subtypes, suggesting that background dependence, number of adaptive mutations, and extent of additive versus epistatic interactions may all be related features of the fitness landscape.

Introduction

Understanding the fitness landscapes of adaptively evolving pathogens, such as influenza virus, by monitoring their natural evolution is often limited by the fact that we can only observe what happened, and not what could have happened. In other words, by just examining the actual evolutionary trajectory, it is difficult to assess how many possible adaptive pathways were available to the virus and the contingencies of evolution that could influence these pathways. These features of the fitness landscape offer insights about the constraints on evolution.

Here, we analyze what happens when a variety of influenza strains are subjected to the same evolutionary pressure. From this repeated "experiment", we use strains with different sequences

1 to observe how the background genotype influences possible modes of adaptation and strains
2 with identical sequences to address how many of these different evolutionary pathways are
3 available to a given virus. Specifically, we examine adaptation of human influenza virus to
4 chicken eggs.
5
6 The majority of the influenza vaccine doses are grown in chicken eggs (Francis et al. 1945)– a
7 practice that was originally developed for military use in response to the devastating 1918
8 pandemic, and was approved for civilian use in 1945 (Anon). Almost immediately it became
9 clear that the vaccine needed to be reformulated to maintain efficacy against viral antigenic
10 evolution (though the exact cause was not appreciated at the time) and by 1952 the Global
11 Influenza Surveillance and Response System (GISRS) was founded to monitor circulating
12 viruses(Hay and McCauley 2018). As a result of GISRS's efforts, we have sequences of the 3
13 seasonal influenza strains that circulate today (A/H3N2, A/H1N1pdm and B/Vic), as well as
14 B/Yam (which recently went extinct in 2020) for the past several decades. These sequences
15 include both direct clinical isolates of the virus and virus that was grown in chicken eggs to
16 produce vaccine.
17
18 This temporal collection of sequences tracks the ongoing evolution of influenza viruses in the
19 human population, a process largely driven by antigenic drift. Simultaneously, the egg-passaged
20 sequences reveal the consequences of introducing this changing virus into a different selective
21 environment, namely growth in chicken eggs. In essence, the egg-passaged sequences
22 represent the result of an evolutionary experiment repeated hundreds to thousands of times.
23 During this experiment, we can observe genetic adaptations of the virus as it experiences a
24 relaxation of pressures to maintain human-to-human transmission (including lack of airborne
25 transmission, absence of existing adaptive immunity, and decreased requirement for acid
26 stability to name a few) in addition to a demand for binding different cellular receptors.
27
28 Influenza initiates cell entry when its hemagglutinin protein binds to sialic acid moieties
29 decorating cell surface proteins and lipids. Human airways express primarily α2,6-linked sialic
30 acid, while the egg allantoic cavity (where virus is grown) contains α2,3-linked sialic acids.
31 Additionally, human influenza viruses typically bind receptor in the cis conformation, while avian-
32 adapted viruses bind in trans conformation. This difference is known to select for egg-adaptive
33 mutations near hemagglutinin's receptor binding pocket that increase the virus' ability to engage
34 α2,3 sialic acid, often at the expense of worse binding to α2,6.
35
36 Because the majority of neutralizing antibodies block viral growth by binding to the receptor-
37 binding region of HA (and thus prevent cell entry), mutations that are selected for during egg-
38 passaging can also incidentally affect the antigenicity of the virus. This means not only that the
39 virus grown in eggs can differ from the vaccine strain carefully selected by the WHO, but also
40 that these differences can impact how the virus is recognized by human antibodies (Raymond et
41 al. 2016). Low vaccine efficacy has been attributed to egg-adaptation in the 2012-2013
42 (Skowronski et al. 2014) and 2016-2017 (Zost et al. 2017) seasons, particularly for the H3N2
43 component of the vaccine where egg-adaptive mutations have been shown to have the largest
44 impact on immunogenicity (Liu et al. 2024).

2

1
2 Many egg-adaptive substitutions have been described in the receptor-binding domain (RBD) of
3 H3N2 (Jin et al. 2005; Lu et al. 2006; Widjaja et al. 2006; Chen et al. 2010; Parker et al. 2016;
4 Wu et al. 2019), H1N1pdm (Suptawiwat et al. 2013; Garretson et al. 2018; Liu et al. 2018; Erin
5 Azbazdar et al. 2022), and the human influenza B viruses (Chen et al. 2008; Wilson et al. 2022).
6 Wu et al (Wu et al. 2019) and Liang et al (Liang et al. 2022) have also shown how epistatic
7 interactions in the RBD of H3N2 influence egg-adaptive mutations.
8
9 Here, we aim to expand on the evolutionary insights that can be gleaned from the thousands of
10 sequences resulting from growing human influenza isolates in chicken eggs. We take
11 sequences of all available egg-passaged strains and situate them in the context of circulating
12 human virus to determine mutations that occurred during egg-passaging. We do this for all 8
13 segments of the 4 human influenza viruses (A/H3N2, A/H1N1pdm, B/Vic and B/Yam). We then
14 separate likely adaptive mutations from those found at consensus level due to genetic drift by
15 finding mutations that occurred frequently amongst strains that were independently passaged in
16 eggs. We also consider how different genotypes of human influenza preferentially adapt to egg
17 passaging via different mutations, as well as pairwise epistatic effects between egg-adaptive
18 mutations. We find that the four influenza subtypes differ in their evolution in eggs, and explore
19 what these differences might suggest about the fitness landscapes of these four viruses.
20 Additionally, we assess the number of possible adaptive trajectories available to a given viral
21 genotype, demonstrating the effects of constraint and stochasticity on adaptation.
22

23 Results

24 Inference of mutations that occurred during egg-passaging

25 For each influenza subtype, we downloaded all available egg-passaged sequences dating back
26 to 1995, encompassing 30 years for A/H3N2 and B/Vic, 15 years for A/H1N1pdm (which
27 entered the human population in 2009), and 25 years for B/Yam (which went extinct in 2020).
28 We refer to each human viral isolate, e.g. A/Massachusetts/18/2022, as a strain (meaning it is
29 possible for multiple strains to have the same genotype) and, for this analysis, we use one egg-
30 passaged sequence per strain, where available. This ranged from a minimum of 570 egg-
31 passaged strains for B/Yam to a maximum of 1901 egg-passaged strains for A/H1N1pdm. To
32 determine what mutations occurred during egg-passaging, one could simply compare the
33 sequence of the strain before and after egg-passaging. However, only 37-67% (Figure 1E) of
34 egg-passaged strains were also sequenced prior to egg-passaging. To make use of all of the
35 data, rather than only the egg-passaged strains with available unpassaged sequences, we built
36 phylogenies for each of the 8 segments in the viral genome, positioning egg-passaged strains
37 strains in the context of the circulating human viruses (Figure 1A-D, non-HA segments available
38 at https://nextstrain.org/groups/blab/h3n2/na/egg). This allows us to determine the likely
39 sequence of each strain prior to egg-passaging from the sequence at the internal node
40 ancestral to it in the phylogeny and, thus, to infer mutations that occurred during egg-passaging

3

1 as those falling on the terminal branch leading to an egg-passaged tip. We can, thus, infer egg-
2 passaging mutations for strains that were sequenced prior to egg-passaging (Figure 1F, tip 1)
3 as well as sequences that were not (Figure 1F, tip 3). Because each egg-passaged strain is a
4 separate instance of a human influenza virus being passaged in eggs, we assume that small
5 clades of only egg-passaged strains are actually polytomies.
6
7 As a form of validation, we compare our list of inferred mutations to a list of all mutations that
8 would be found via direct comparison of egg-passaged strain and its unpassaged pair
9 (Supplemental Figure 1). We find that the inferred and "known" mutations agree for all
10 commonly observed egg-passaging mutations (in fact, for all mutations that occur in 1% or more
11 of egg-passaged strains). Thus, the inferred mutations that were not directly observed between
12 pairs are rarer mutations, occurring in just one or a handful of egg-passaged strains, suggesting
13 that these mutations either actually arose in an unsampled human virus or that they are just
14 random (unselected) mutations that arose during egg-passaging.
15

16 ## Egg-adaptive mutations are primarily located near the receptor binding
17 pocket of HA

18 Across the eight segments of all four influenza viruses, we observe that 9-40% of strains
19 acquired synonymous mutations during egg-passaging. Longer segments (PB1, PB2, PA) tend
20 to have synonymous mutations in more strains than shorter segments (MP, NS) (Figure 2A), in
21 accordance with expectations of size of target for random mutation. The proportion of strains
22 with nonsynonymous mutations is highest for the HA segment, reaching 81% of strains for
23 H3N2. Additionally, the HA segments of the four subtypes plus the H1N1pdm NP and H3N2 NS
24 segments are the only instances where the proportion of strains with nonsynonymous mutations
25 exceeds the proportion with synonymous mutations.
26
27 We then zoom in to the locations of the nonsynonymous mutations by tallying the proportion of
28 strains with an amino acid change at each residue across the length of the segment. In general,
29 we see an even distribution of amino acid changes across most segments (Figure 2B),
30 indicating that these substitutions are occurring at random, rather than at functionally-important
31 residues. In stark contrast to the flat topography of these plots for most segments, we see tall
32 spikes within the HA histograms, marking residues that were independently mutated in many
33 strains, and suggesting that amino acid changes at these positions have been selected for.
34
35 Each egg-passaged strain in this analysis is the result of passaging a different strain in chicken
36 eggs, meaning that we have not included multiple sequences of serial passages of the same
37 strain. Therefore, each sequence is an independent recounting of the evolutionary consequence
38 of growing human influenza virus in chicken eggs. Because of this, the number of times a
39 particular mutation is observed in different strains is reflective of its selective coefficient. In other
40 words, a mutation occurring just once across hundreds of egg-passaged strains is likely
41 evolutionarily neutral in this context, while a mutation that appears in many strains has likely

4

1 been selected for due to a fitness advantage in the face of pressure common to all of these
2 strains, i.e. growth in chicken eggs.
3
4 Using this logic, we separate egg-adaptive mutations from neutral and deleterious mutations by
5 the number of times they occur amongst all egg-passaged strains. Specifically, we pick out
6 residues that were mutated in at least 2.5% of egg-passaged strains overall, or specific
7 substitutions that reach at least 7.5% within a 3-year window. We picked this threshold to
8 substantially exceed 1%, thereby excluding any potential false positive egg-passaging
9 mutations (Supplemental Figure 1). We believe this threshold is fairly conservative, allowing us
10 to be confident that the mutations we have identified are truly adaptive, but at the cost of likely
11 missing some mutations with only a small beneficial effect. By this metric, all putatively egg-
12 adaptive mutations occur in HA or NP.
13
14 We identify residues with egg-adaptive mutations within the HA segment of all four viruses
15 (Figure 2C-F). Every one of these sites is located within the receptor-binding domain of HA1,
16 and most of them are found within structural features of the HA protein that surround the
17 receptor-binding pocket (130-loop, 150-loop, 190-helix and 220-loop). The influenza B adaptive
18 mutations are primarily focused in the 190-helix, while the influenza A (especially H3N2)
19 mutations are more spread out between these features. In fact, all of the Vic adaptive mutations
20 occur at structurally homologous positions to the Yam mutations, and the amino acid
21 substitutions observed amongst adaptive mutations are also almost identical (Supplemental
22 Figure 2). The influenza A viruses share two structurally homologous loci of egg-adaptation in
23 the 190-helix and another two in the 220-loop, again, getting mostly the same amino acid
24 substitutions. The four egg-adaptive residues shared between H3N2 and H1N1pdm were also
25 identified by Dadonaite et al (Dadonaite et al. 2024) as being crucial for α2,3- versus α2,6-sialic
26 acid binding in H5 viruses.
27
28 Highlighting the egg-adaptive sites on the structure of HA emphasizes the proximity of these
29 residues to the receptor-binding pocket (Supplemental Figure 3). The striking enrichment of
30 mutated sites flanking the receptor-binding pocket of these viruses suggests that there is strong
31 selection for protein change at the interface of hemagglutinin and the sialic acid receptor, likely
32 to improve binding of the altered conformation of these sugars presented by avian egg cells
33 compared to human respiratory cells. Some of these mutations are known to directly impact
34 binding of human versus avian sialic acid (Suptawiwat et al. 2013; Wu et al. 2019; Powell et al.
35 2021), while others have been noted to abolish glycosylation (Robertson et al. 1985;
36 Gambaryan et al. 1999; Wang et al. 2007; Zost et al. 2017). Egg-adaptive mutations that
37 prevent glycosylation include the 196/198 (or 195/197) mutations in Vic (or Yam), and the H3N2
38 mutations at 160 and 246. Though we cannot determine the reason mutations that remove
39 glycans from HA1 are selected for in eggs, it seems likely that either these glycans compromise
40 binding to α2,3-sialic acid and/or a pressure to retain glycans as a defensive shield against
41 human neutralizing antibodies is relaxed.
42
43 We also detect a few potentially adaptive mutations in the nucleoprotein (NP) segment of both
44 influenza A viruses (Supplemental Figure 4). H3N2 viruses have two residues in NP that are

repeatedly mutated during egg-passaging (290 and 384), while H1N1pdm strains have three sites (101,102 and 375), including two neighboring residues. Fitting with a potential role in host adaptation, all 5 of these residues are found amongst the sites that Kukol and Hughes identify as varying most between hosts (Kukol and Hughes 2014). Though it may be expected that egg-adaptation in NP would result in reversion mutations that revert the protein back from human-adapted to avian adapted. The NP segment of both H3N2 and H1N1pdm was introduced from avians to humans in the 1918 H1N1 pandemic and was subsequently transferred multiple times through different subtypes and different species via reassortment. We, therefore, compare the egg-adaptive NP mutations to a 1918 H1N1 NP sequence (Genbank AY744935) and find that only one (H3N2 G384R) of the five mutations we identify is a reversion.

The NP protein is essential for transporting viral RNA into the nucleus for replication (O'Neill et al. 1995), a process that relies on interactions with importins and other host cell machinery that differ between humans and birds (Gabriel et al. 2011). However, the positions where we observe mutations do not fall within NP's nuclear localization sequences (Cros et al. 2005), indicating that egg-adaptation may be through a different mechanism. Chen et al (Chen et al. 2006) also found that nucleoprotein has the most positions out of any segment that act as signatures for differentiating human from avian influenza strains, but the mutations we observe are also not amongst these sites.

The circulating human influenza genotype influences which egg-adaptive mutations can occur

Human influenza viruses have undergone a considerable amount of antigenic evolution during the past 30 years and, as with egg-adaptation, antigenic evolution is also focused in the receptor-binding domain of HA1. Thus we expect that egg-adaptive mutations will change over time as the human virus evolves, either due to the human virus incidentally becoming more or less fit in eggs or because of epistatic constraints of the HA structure. Plotting the prevalence of mutations at each adaptive residue over time reveals that some mutations to some sites are temporally restricted (e.g. H3N2 225 and H1N1pdm 191), while others are not (e.g. H1N1pdm 223 and Yam 195) (Figure 3, left). Additionally, at sites where we observe adaptive changes to multiple different amino acids, we again see that some substitutions, such as H3N2 194I vs. 194P, are time-dependent while others, like H3N2 219F vs. 219Y, are not (Figure 3, right).

Figure 3 reveals differences in the time dependence of egg-adaptive mutations between the different influenza subtypes. Though some mutations are observed for a decade or longer while others are confined to just a handful of years, we observe temporal restriction for every single H3N2 egg-adaptive site, and among many of the specific adaptive substitutions at these sites as well. The other influenza A virus, H1N1pdm, has some egg-adaptive mutations that are prominent across the entire time frame (223R and 222G/N) while the mutations at the other three sites occur only during a section of time. It should be noted that this analysis spans 30 years for H3N2 and only 15 years for H1N1pdm, and it is possible that H1N1pdm 222 and 223 mutations will not continue to be egg-adaptive on a longer time scale. In contrast to the

6

influenza A viruses, influenza B/Yam shows no time dependence, and the dominant B/Vic sites (196 and 198) get mutated regularly and consistently until around 2020 when mutations to both sites stop appearing.

Time dependence of egg-adaptive mutations is a proxy for dependence on the genotype of the human influenza virus that was passaged in eggs. To determine which genetic changes that occurred during the evolution of these influenza viruses as they circulated in humans subsequently impacted egg-adaptation, we identified HA1 substitutions occurring on the trunk of the tree that correspond best with presence or absence of a particular egg-adaptive mutation. We are able to identify genetic changes in the human virus that correlate with many of the time-restricted egg-adaptive mutations. Based on these results, we classify the genetic dependence of egg-adaptive mutations on human genotype into three main categories that likely explain the time-dependence: 1) fixations in the human virus that alter fitness in eggs, 2) mutational codon accessibility, and 3) epistatic interactions between the adaptive mutations and the background. The first category includes mutations like H3N2 186 and Vic 196 mutations (Figure 4), where the human virus fixes substitutions at the egg-adaptive site, resulting in multiple genotypes with potentially different fitnesses in eggs.

As seen in Figure 4A, human H3N2 had a serine at position 186 until around 2000, when 186G swept. We observed no egg-adaptive mutations on top of 186S (encoded by codon AGT), even though the highly-adaptive 186N is accessible via a single nucleotide mutation, indicating that 186S has high fitness in eggs. Once 186G sweeps, we begin to see frequent mutations to 186V during egg-passaging, with as many as 63% of egg-passaged strains during a single year (2013) getting 186V (Figure 3A). During this time period, there are also a handful of egg-passaged strains that get 186S, again pointing towards 186S being fairly high fitness in eggs. The vast discrepancy between the number of egg-passaged strains that get G186V vs. G186S speaks to valine being even more beneficial for egg growth than serine during this time period. The 186N mutation was not available during this time period, but following the subsequent fixation of 186D in the human virus, both egg-adaptive mutations (186N and 186V) become accessible via a single nucleotide mutation. During this time period, 38% of the 245 egg-passaged strains get the 186N mutation while 186V occurs in just 5 strains. In the absence of epistatic influences from other sites throughout RBD, this suggests that H3N2 has a preference for N, then V, then S at 186 when grown in eggs, and that G and D have fairly low fitness, though epistasis likely does complicate this conclusion.

We can similarly work out the relative fitnesses of different genotypes at other HA1 positions based on the genotype of the human virus and the occurrence and identity of observed egg-adaptive mutations. For instance, the circulating human Vic virus has 196N (encoded by the AAC codon) from 1994 until around 2020, and every observed egg-adaptive mutation at 196 occurs during this period. Around 2020, 196D fixes in the human population and egg-adaptive mutations at this site cease, which makes sense because 196D is actually one of the observed egg-adaptive mutations, further suggesting that 196N has lower fitness in eggs than 196D. After a matter of just a couple years, the circulating virus again fixes a 196 mutation, changing the human virus to 196E (encoded by GAA). Though 196E is not an egg-adaptive mutation we

observed, we suggest that it is also high fitness in eggs because we observe only a single egg-adaptive mutation on human strains with 196E, despite the fact that both D and K adaptive substitutions are mutationally accessible. We suggest that the reason E is not observed after egg-passaging during the long span of time when egg-adaptive mutations are occurring on 196N is because E requires two mutations from AAC (encoding N), whereas the other adaptive mutations are accessed by just one.

With H3N2 193R, we see a strong example of how mutational distances between codons can impact whether or not an adaptive mutation will occur. Until around 2004, circulating human H3N2 had a serine encoded by AGC at residue 193, and during this period we observe several egg-passaged strains mutating to 193R during this period. However, in the ensuing years, a couple nucleotide mutations fix in the 193 codon, resulting in a sweep of phenylalanine and then a reversion to serine. The serine reversion is encoded by TCC, which is now two mutational steps away from R, emphasizing that despite evidence that 193R is preferred over 193S in eggs, it will not occur due to mutationally accessibility. The reason accessibility matters so much is because a substitution requiring two mutations would either need to get both precise mutations simultaneously (which is very unlikely) or acquire a first mutation followed by the second (which is also very unlikely since the first mutation would not be selected for). Finally, we also see that some egg-adaptive mutations are impacted by epistatic interactions with other sites in the HA protein (Figure 5). An example of this is H3N2's egg-adaptive 194P mutation, whose occurrence is bounded tightly by a phenylalanine at position 193 in the human virus. We see 194P occurring exclusively on top of 193F, and never on 193S. This includes a couple of small clades with 193S in the 2010's that never developed 194P mutations when passaged in eggs, while their sister clades with 193F did.

The H1N1pdm 191I mutation occurs in eggs from 2009 until 2017-2018, around which point egg-adaptive mutations at residue 187 started occurring (Figure 3B). This switch coincides with a S-to-P fixation at position 183 in the circulating human virus. Of the 86 egg-passaged strains with a 191I mutation, all but two occur in human strains with 183S, and of the 125 egg-passaged strains that acquired 187V/N/T mutations, 100% occur on top of 183P (Figure 5). Both 187 and 191 are located on the side of the 190-helix facing the receptor-binding pocket whereas 183 is located in the loop preceding this helix. Because prolines limit rotation around the protein backbone, we hypothesize that the S183P fixation may alter the position of the 190-helix such that mutations at residue 191 are no longer able to improve receptor-binding to α2,3-linked sialic acids, and instead, mutations at 187 become important for this function. In support of this theory, the equivalent residue H3N2 (186) is a major site of egg-adaptation and a mutation from G to V at this site was shown to shift the location of the 190-helix, thereby expanding the receptor-binding pocket (Wu et al. 2019).

8

Epistasis between egg-adaptive mutations influences the length of adaptive trajectories

We next consider how the mutations acquired during influenza's pursuit of egg-adaptation are influenced not just by the genotype of the human virus injected into the egg, but also by the presence of other egg-adaptive mutations. For each pair of egg-adaptive mutations in HA1, we calculate an enrichment ratio to determine whether the mutations co-occur more or less often than would be expected from the individual frequencies of the two mutations. To account for background dependency, we require that the period of time the two mutations are observed must overlap by at least three years. As seen in Figure 6A, the H3N2 plot has both many grey boxes- recapitulating strong background dependency of H3N2 mutations shown by Figure 3A- and many more red boxes, indicating that egg-adaptive mutations co-occur more commonly in H3N2 than they do in H1N1pdm or influenza B viruses. In fact, egg-adaptive mutations never co-occur in influenza B viruses (Figure 6C-D). In egg-passaged H1N1pdm viruses, there is also a dearth of co-occurring adaptive mutations, with the neutral enrichment scores primarily being observed between mutations at 222 and another residue (Figure 6B).

The mutually exclusive nature of egg-adaptive mutations in Vic and Yam indicates that as human influenza B virus adapts to eggs, it has access to at least 3 distinct fitness peaks, separated by sign epistasis. The source of this epistasis could either be because the mutations are structurally incompatible or because they have completely non-additive beneficial effects. In the latter case, it would be possible that the mutations have completely overlapping effects or that their mechanisms of adaptation are actually antagonistic to each other. Both of the mutations in the 190-helix act to remove the same glycan, so the presence of one of these adaptive mutations drops the effect of the other to neutral, or even deleterious. It is difficult to tell from these data why 141R does not co-occur with either 190-helix mutation.

In contrast, the pairwise co-occurrence of some H3N2 mutations with each other suggests that egg-adaptation in this virus can be achieved through the additive, or even synergistic, effects of multiple mutations. In particular, we see that some adaptive mutations like 138S, 160K/I and 225G/N co-occur with other mutations frequently while others, like 246K and 186N do not. The fixation of multiple adaptive mutations in the same strain suggests either that the mutations have distinct, non-overlapping beneficial effects for the virus, or that mutations actually have similar molecular benefits that can act in coordination. Others have provided evidence that both of these are at play in H3N2 egg-adaptation. The mutations at residue 160 remove a glycan and it is likely that the advantage of this is independent of mutations that alter the receptor-binding pocket itself. On the other hand, the combination of 186V and 226I increased viral growth in the egg allantois where neither mutation alone did, implying a synergistic effect of these mutations (Widjaja et al. 2006).

However, negative epistasis also creates distinct fitness peaks during H3N2 egg-adaptation. Figure 6A shows a depletion of 186N co-occurring with 195Y mutations. Circulating human H3N2 had a tyrosine at residue 195 until phenylalanine fixed around 2020. After this point, 186N

1 mutations and reversions to 195Y both become frequent in egg-passaged strains, occurring in
2 94/275 and 29/275 of the egg-passaged strains derived from unpassaged strains with 195F,
3 respectively. However, these mutations only occur together in the same strain twice, indicating
4 that 186N and 195Y both strongly increase fitness in eggs but that their benefits are not
5 additive. Similarly, 186V and 194P mutations are both very common from 2005-2019, but are
6 never found simultaneously. Wu et al (Wu et al. 2019) have shown that mutual exclusivity of
7 these highly adaptive mutations is due to a structural incompatibility. These results suggest that,
8 like for influenza B viruses, the fitness landscape of egg adaptation by human H3N2 also has
9 multiple peaks separated by sign epistasis but, unlike influenza B viruses, the H3N2 peaks
10 contain longer adaptive walks consisting of multiple adaptive mutations, rather than just one.
11
12 This trend toward longer adaptive trajectories (or more mutational co-occurrence) in H3N2 is
13 again evident when assessing the total number of adaptive mutations per egg-passaged strain
14 (Figure 6E). Of H3N2 strains that get adaptive mutations in HA1 during egg-passaging, 48% of
15 them get multiple, with some strains getting 3, 4 or even 5 adaptive mutations. This is in stark
16 contrast to 4% of H1N1pdm strains that get 2 mutations and 0% of Vic or Yam getting multiple
17 egg-adaptive mutations.
18
19 If we view H3N2 and the influenza B viruses as having different modes of egg-adaptation with
20 regards to epistasis between adaptive mutations and the length of adaptive trajectories,
21 H1N1pdm is somewhere in between.
22

Egg-adaptation of human influenza virus reveals many possible adaptive trajectories

25 The sign epistasis we observe in Figure 6 suggests that a given influenza hemagglutinin protein
26 can access multiple available pathways towards egg-adaptation. Figures 3 and 4 demonstrate
27 that the pathways available to a given hemagglutinin change over time due to background
28 dependence for H3N2 and to some extent H1N1pdm but very little for influenza B strains. This
29 suggests that, amongst egg-passaged strains derived from identical unpassaged strains, we will
30 not observe exact repetition of egg-adaptation, but rather an assortment of the different adaptive
31 mutations available to that background. To test this more directly, we compare egg adaptation
32 between sets of strains that have identical HA1 sequences before egg-passaging. We identify
33 37 sets where at least 5 egg-passaged H3N2 strains derive from the same unpassaged HA1
34 sequence (48 H1N1pdm sets, 34 Vic sets, and 23 Yam sets).
35
36 Indeed, we see that when a virus with a given HA1 sequence is passaged in eggs many times
37 in parallel, the virus will not adapt to eggs via the same adaptive pathway each time. For
38 H1N1pdm and influenza B viruses, we see many examples where the same HA1 sequence will
39 develop each of the possible egg-adaptive mutations in independent replicates (Figure 7A,
40 Supplemental Figures 5-8). Again, we observe only single adaptive mutations occurring in
41 influenza B viruses and just a handful of H1N1pdm viruses with two egg-adaptive mutations. For
42 H1N1pdm, we observe that HA1 sequences that have access to an adaptive mutation at

residue 187 do not have access to 191 and vice versa. In general, the number of different adaptive mutations observed within a set increases with the number of strains in that set (Figure 7B). This supports our hypothesis that each of these influenza viruses have access to multiple mutually exclusive egg-adaptive pathways, and which mutation fixes will depend on the relative selective coefficient of that mutation and, importantly, to stochasticity of the mutation occurring.

The H3N2 sets reflect a higher degree of background dependence as noted in Figures 3 and 4, with only a subset of adaptive mutations appearing amongst the egg-passaged strains in each set. There are several H3N2 sets where many viruses fixed the same mutation, but some viruses also got an additional mutation or two, suggesting incomplete evolution down a shared adaptive pathway. Perhaps if the viruses were grown in eggs for longer, the results of egg-adapted H3N2 viruses would converge even more. Potentially incomplete adaptation, strong background dependence, and H3N2's faster rate of evolution in humans (resulting in smaller set sizes, on average) could all contribute to the observation that we never see H3N2 sets with mutations at every site that is observed amongst all egg-passaged strains during the same time period. This is shown by Figure 7B, where in contrast to H1N1pdm, Vic and Yam, all H3N2 sets fall below the dashed line.

Being able to look at repetition of the same hemagglutinin sequence adapting to chicken eggs over and over again gives us a unique view into what the possibilities of evolution are. In other words, we can infer that an H1N1pdm strain that adapted to eggs via a 191I mutation could have instead adapted via a mutation at 127, 222, or 223, and the fact that 191I is what occurred is due, in large part, to stochastic effects. With this framing, we can consider the differences between avian influenza A and human influenza A viruses. We hypothesize that egg-adaptation should mirror differences between human and avian HA that enable them to better bind α-2,6 versus α-2,3-sialic acids.

For H1 and H3, we compare the genotypes observed in human and avian influenza at each egg-adaptive site. We notice that, at most sites, the egg-adaptive amino acid is not what is observed in avian influenza, and in fact, that avian and human HAs often have the same or similar amino acids at these sites (Supplemental Figure 9). However, avian H1 has 127E and the highly egg-adaptive 222G and avian H3 has genotypes 186S, 195Y, 225G that we observe to be egg-adaptive. We speculate that these sites represent the different pathways avian and human influenza hemagglutinin evolution have actually taken to recognize α-2,3 versus α-2,6-sialic acid, while the results from our egg-adaptation analysis represent alternative evolution that could have taken place to differentially allow these hemagglutinins to better bind the sialic acids of their host species.

Notably, the human H3N2 virus has fixed each of these egg-adaptive mutations that are found in avian H3 (186S, 195Y, and 225G) at different points during the past 30 years (Supplemental Figure 9). This is not the case for H1N1pdm: we don't observe egg-adaptive mutations fixing in the human virus population. This suggests that during its ongoing evolution in humans, the human H3N2 virus incidentally becomes more and less able to bind avian α-2,3 sialic acid, a

11

1 hypothesis supported by a fluctuating total number of adaptive mutations over time

2 (Supplemental Figure 10).

Discussion

4 In the study of viral evolution, say that of influenza viruses, we know stochasticity and historical

5 contingency are influential forces, yet we are often limited to scrutinizing what did happen, and it

6 is much harder to assess what could have happened. This leaves open important questions

7 regarding how determinative versus stochastic adaptive evolution is; does the virus have 100s

8 of possible adaptive trajectories? Tens? A couple? One? Natural populations of human viruses

9 are under a wide and changing range of selective pressures, making it quite complicated to

10 determine all of the possible evolutionary trajectories. Here, we looked at a less complicated

11 and more tightly bounded selective regime: adaptation of human influenza virus to chicken

12 eggs. By assessing repeated evolution in this situation, we found that human influenza virus has

13 a handful of different adaptive trajectories toward egg-adaptation, that these trajectories change

14 as the human virus evolves, and that all of this differs between the four human influenza

15 subtypes.

16

17 We find that, during egg-adaptation, influenza subtype A/H3N2 exhibits the most background

18 dependence, the most positively-epistatic interactions, and the longest adaptive walks. In all of

19 these aspects, A/H1N1pdm ranks second, followed by the two influenza B subtypes, which

20 adapt very similarly. These findings are consistent with at least two different (non-mutually

21 exclusive) hypotheses to explain the differences in egg-adaptive evolution between the

22 subtypes: 1) human influenza B viruses are more fit in eggs, and/or 2) human influenza A

23 viruses (and particularly H3N2) have more adaptable hemagglutinin proteins. In support of

24 hypothesis 1, more possible adaptive mutations and longer adaptive walks (as seen in H3N2)

25 are characteristics of a population further from a fitness peak, while mutually exclusive adaptive

26 mutations mediated by sign epistasis (like Vic and Yam) are characteristic of a population close

27 to a fitness peak (Fisher 1930; Smith 1970; Moutinho et al. 2022). This hypothesis seems quite

28 plausible except that influenza A viruses (including H3NX and H1NX) are prolific in wild bird

29 populations, while birds are not a natural host of influenza B viruses. On the other hand, some

30 proteins are known to be more generally tolerant to mutations than others, and it is possible that

31 the influenza A hemagglutinins are more flexible in a way that allows them to more easily fine-

32 tune the receptor-binding pocket to accommodate different sialic acids. Interestingly, this same

33 ordering of subtypes also describes their relative rates of antigenic drift (Bedford et al. 2014;

34 Kistler and Bedford 2023), offering the possible hypothesis that this H3 hemagglutinin has more

35 mutational flexibility in the receptor-binding pocket, which allows it to more readily adapt to α2,3

36 receptors and also to more readily access antigenic variation that does not compromise

37 receptor-binding. If this hypothesis is true, we should also observe faster adaptation of H3

38 compared to H1 in other contexts, such as in other species. However, we do not find evidence

39 of ongoing adaptation within avian viruses (Supplemental Figure 11) and therefore cannot make

40 this comparison between avian HAs. From our results, we cannot distinguish between the

41 potential explanations of the different egg-adaptation observed between influenza subtypes.

42

We also find that the total number of egg-adaptive sites varies more over time for A/H3N2 than it does for the other viruses (Supplemental Figure 10). This result aligns with H3N2's higher background dependence (Figures 3 and 4), and suggests that evolution of human H3N2 brings the virus into different regions of the fitness landscape in eggs. The ongoing antigenic evolution in humans incidentally makes the virus more or less fit when it is subsequently passaged in chicken eggs, and also can alter available pathways towards egg-adaptation (Figures 3-7). Importantly, faster antigenic evolution (which alters the background), alone, cannot fully explain the higher number of egg-adaptive mutations observed among H3N2, then H1N1pdm, then influenza B viruses because we observe this trend amongst viral strains with identical sequences (Figure 7B) and because we observe that A/H1N1pdm viruses get more egg adaptive mutations than B/Vic viruses despite both accruing a similar number of fixations per year in humans (Supplemental Figure 12).

In the context of a rapidly-evolving protein that fixes ~0.5-3 amino acid substitutions in HA1 subunit each year, we find the degree of parallelism between egg-adaptation of the different influenza subtypes to be quite striking. The influenza B lineages, Vic and Yam, diverged in 1983 (Rota et al. 1990) and since then, their hemagglutinin proteins have been undergoing separate antigenic evolution including fixations at different residues and a deletion in B/Vic (Langat et al. 2017; Virk et al. 2020). Despite this, we observe that both viruses adapt to eggs via similar substitutions at equivalent residues (Supplemental Figure 1). The human influenza A subtypes are estimated to have diverged hundreds or thousands of years ago (Suzuki and Nei 2002) yet they share several prominent sites of egg-adaptation (Supplemental Figure 1), and these sites were also shown to contribute to α2,3 versus α2,6 receptor preference in H5 (Dadonaite et al. 2024) and H7 (Shi et al. 2013). These positions are not conserved between HA types, or even within them. This suggests that despite many fixations at these positions and throughout the receptor-binding domain, the evolutionary constraints acting on the hemagglutinin protein have maintained receptor-binding pockets that are similar enough in structure and mechanism to be able to alter binding preference via similar mutations.

In this work, we draw on repeated patterns during independent evolutions of human influenza virus to chicken eggs to infer patterns underlying this adaptive landscape. Because of this we are blind to strain-specific effects. For instance, if there is just a single egg-passaged strain available within a small clade of human virus, we will not infer mutations private to that egg-passaged strain to be adaptive, even though it is possible that they represent bona fide egg-adaptation that is specific to that rare background. This causes us to potentially underestimate the number of egg-adaptive pathways in areas of the human virus phylogeny where egg-passaged sequences are sparse. This is a compromise we make to be confident that the mutations we are analyzing have a true adaptive function.

Another limitation of this work is that there is variation in the number of times the different strains were passaged in eggs, and thus in the amount of evolutionary time they had to adapt. This could result in egg-passaged strains that are at an intermediate point in their adaptation (as hinted at in Figure 7). This complicates direct comparisons of individual strains, but again we draw power from comparing hundreds or thousands of strains. Given more passaging time, we

13

1 would likely see a higher total number of strains with adaptive mutations, more mutational co-
2 occurrence, and potentially a few more adaptive mutations with smaller (or more background-
3 dependent) selection coefficients. However, this is unlikely to change the conclusions about
4 egg-adaptation or its variance between subtypes that we discuss throughout this paper.
5

6 Here, we have looked to repeated adaptive evolution as a way of assessing the fitness
7 landscape by using reiterated patterns of mutational co-occurrence to infer peakedness and
8 epistatic constraints. Another common way to do this is by employing deep mutational scanning
9 (DMS) to exhaustively determine the effect of every combination of mutations (Weinreich et al.
10 2006; Dawid et al. 2010; Papkou et al. 2023; Judge et al. 2024). This strategy has the benefit of
11 directly measuring the effect of all pairwise mutation combinations, however it is limited both to
12 phenotypes that are easily measurable in large-scale laboratory experiments and to a relatively
13 small number of interacting sites. For instance, Wu et al (Wu et al. 2017) work out epistatic
14 interactions between 11 residues in the HA receptor-binding site by quantifying the fitness effect
15 of all pairwise combinations of amino acids, but extending this experiment to all of HA1 would
16 be intractable (>19 million variants). With the goal of pushing our understanding of viral
17 evolution past the effects of individual mutations on specific strains toward a more
18 comprehensive view of the adaptive seascape the virus is evolving on, we view observation of
19 natural evolutionary replicates as a complementary approach to exhaustive mutagenesis
20 coupled with experimental phenotype measurement, with each method offering different
21 advantages and insights.

Acknowledgements

Methods

29 All code associated with the analyses in this manuscript is hosted at:
30 https://github.com/blab/egg-adaptation.
31

Sequence data and phylogenetic tree enriched in egg-passaged strains

34 Sequence data for all egg-passaged seasonal influenza strains was downloaded from GISAID
35 separately for each segment (PB1, PB2, PA, HA, NP, NA, MP, NS) of seasonal influenza virus
36 (H3N2, H1N1pdm, Vic and Yam) separately. We then filtered this data to include only one egg-
37 passaged sequence per strain. Some strains that were passaged in eggs have been sequenced

14

multiple times after different numbers of passages (and/or by different labs), and we chose to include the strain that was passaged the most number of times. We downloaded these sequences on March 31, 2025 and took only sequences between then and 30 years prior to this date. We then downloaded non-egg-passaged sequences for each segment and virus and subsampled them to ~10000 sequences sampled as evenly as possible over this 30 year time window and over geographic regions. Within these sequences, we include all available non-egg-passaged sequences of each of the egg-passaged strains (referred to as "pairs" in Figure 1E). We combined the egg-passaged strains and the contextual non-egg-passaged strains together to form the dataset which we used to build the phylogeny with a Nextstrain pipeline. All sequences were aligned to a reference strain (H3N2 = A/Aichi/2/1968, H1N1pdm = A/California/07/2009, Vic = B/Russia/1969, Yam = B/Yamagata/16/1988) using Nextclade3. Trees were built using iqtree. During tree building, nucleotide sites that commonly mutate during egg-passaging were masked with an N so that they did not influence the topology. The masked sites (relative to the reference coordinates) were: H3N2 HA 556, 633, 634, 658, 750, and 751, H1N1pdm HA 631, 642, 735, 736, and 739, Vic HA 665, 666, 670, and 671, Yam HA 645, 646, 647, 651, and 652. All sites were then unmasked and TreeTime was used to estimate dates and sequences of internal nodes and assign mutations to them. Subsequent to exporting trees into auspice JSONs, we broke clusters of egg-only sequences into polytomies. These egg-enriched influenza trees can be viewed here https://nextstrain.org/groups/blab/h3n2/ha/egg, and the subtype and segment in the URL can be changed to view all 32 subtype and segment combinations. Acknowledgements for the labs that generated the sequences used in this study can be found in tabular format at https://github.com/blab/egg-adaptation/nextstrain_builds/gisaid_acknowledgements/gisaid_acknowledgements.tsv.

Egg-passaging mutation and adaptive substitution inference

All mutations that occurred during egg-passaging are inferred to be those occurring on terminal branches leading to egg-passaged strains. For each influenza virus and each segment, we store a list of all egg-passaging mutations that occurred for all egg-passaging strains inferred from the phylogeny in the folder `egg-mutation-analysis/egg-muts-by-strain/`. We also store a summary of the total number of egg-passaged strains, the frequency with an egg-passaged mutation, frequencies of all specific egg-passaged substitutions and of mutations to all residues, as well as a list of mutations that exceed 1%, 2.5%, and 5% of egg-passaged strains in `egg-mutation-analysis/egg-mut-counts/`.

We then infer probable adaptive substitutions for each segment of each subtype as those that occur independently in at least 5 different strains and where a) at least 2.5% of egg-passaged strains have an egg-passaging mutation at that residue, or b) at least 7.5% of egg-passaged strains within a 3-year window have that exact substitution. Adaptive mutations are calculated in `egg-mutation-analysis/get_adaptive_muts.ipynb` and stored in JSON files in `egg-mutation-analysis/egg-adaptive-muts`.

Protein structures

For visual representation of the location of egg-adaptive mutations on the hemagglutinin protein, we used solved structures of HA deposited on PDB with the accessions 2YP4 (H3N2) (Lin et al. 2012), 3UBE (H1N1pdm) (Xu et al. 2012), 4FQM (Vic) (Dreyfus et al. 2012), and 4M40 (Yam) (Ni et al. 2013). For the nucleoprotein structures, we used 7NT8 (H3N2) (Knight et al. 2021) and 3ZDP (H1N1) (Chenavas et al. 2013).

Time window analysis

The changing prevalence of egg-adaptive substitutions over time was assessed by apportioning the egg-passaged sequences into overlapping 3 year windows. Within each 3 year window, the proportion of strains with an adaptive amino acid substitution was determined for each residue position in HA1 with adaptive mutations. For each residue position with more than one adaptive amino acid substitution, the proportion of egg-passaged strains with a mutation to the different amino acids was calculated for each year. This analysis is done in `figure_panels/Figure3-timeWindows.ipynb`.

Background genotype correlations with egg-adaptive mutations

For each temporally-restricted egg-adaptive mutation, we used the tree to identify HA1 mutations happening along the trunk that precede the egg-adaptive mutation's appearance, or follow the mutation's disappearance. We then determined which of these trunk mutations correlate perfectly or nearly perfectly with strains containing the egg-adaptive mutation. If multiple trunk mutations had a good correlation with the egg-adaptive mutation, we presume mutations at the same residue are most likely to be responsible for the temporal restriction, and mutations at structurally proximal residues are the next most likely.

Mutational co-occurrence enrichment score

For each influenza subtype, a mutational co-occurrence score was determined for every pair of adaptive mutations that overlap temporally. We define mutation A and mutation B as co-occurring temporally if there are at least 5 of each mutation and 25 A plus B mutations within the intersection of the date range over which A and B are observed. Mutation pairs that do not meet this criteria are considered non-overlapping and are colored grey.

For pairs of mutations that do overlap, we calculate the individual frequencies of mutation A and mutation B as well as the paired frequency of A and B in the time window of overlap. We then compute an enrichment score using the formula $log2\left(\frac{freqA+B}{freqA*freqB}\right)$. Pairs of mutations that never co-occur result in a mathematically undefined value, but represent a severe depletion of co-occurrence. We color these pairs dark blue.

For this analysis, we separate the different substitutions at a given position if the amino acid substitutions change over time (see time window analysis). For instance, H3N2 186S, 186V, and 186N are considered different adaptive mutations for this analysis because they occur during different periods of time, but 156Q and 156R are grouped together because they occur during the same period of time. The code for this analysis is in `figure_panels/Figure5-betweenMutEpistasis.ipynb`.

Sets of egg-passaged strains from identical HA1 sequences

For each egg-passaged strain, the HA1 sequence before egg-passaging is inferred as the sequence at the first internal node in the phylogeny. This is done by applying every mutation along the path between the root and this node to the root sequence. For each strain, the inferred sequence before egg-passaging is stored in a subtype-specific file like `egg-mutation-analysis/before-egg-seqs/h3n2_HA1_seqs_before_egg.json`. All egg-passaged sequences with identical HA1 sequences prior to egg-passaging are determined and grouped into sets of "replicates", which are stored in `egg-mutation-analysis/before-egg-seqs/h3n2_replicate_sets.json`. For each set, a "haplotype" is assigned to each constituent strain within the set, where haplotype refers to which egg-adaptive sites (residues) are mutated in that strain. The number of strains with each haplotype are counted to produce the plots in Figure 7A and Supplemental Figures 5-8, representing egg-adaptation of every replicate within a set.

Avian H1 and H3 phylogenies, for human to avian genotype comparison

All alphainfluenzavirus (NCBI:txid197911) sequences from an avian host were downloaded from NCBI Genbank in FASTA format on June 4, 2024 (n=271,324). HA type was parsed from the metadata, where available, using the custom script `parse_ncbi_fasta.py`, which outputs one FASTA data file per HA type. Using the H1 and H3 files as input, we then ran a Nextstrain pipeline to filter, subsample, and align sequences, and to reconstruct a time-resolved phylogeny and infer mutations across the tree. Specifically, we used `augur filter` to select only hemagglutinin sequences, and to subsample a maximum of 50 samples per year between 1950 and the present. We used `augur align` to align all H1 sequences to A/California/07/2009 (accession: CY121680) and all H3 sequences to A/Aichi/2/1968 (accession:CY121117). These are the same reference sequences we used to generate the human and egg-passaged H1N1pdm and H3N2 trees used throughout this work, ensuring that the coordinate systems are consistent. We then build trees using IQ-TREE and use Treetime to estimate molecular clock branch lengths, rooting on an outgroup sequence. We root H1 on the avian H3 A/mallard/Wisconsin/418/1976 HA sequence (accession: CY180420) and H3 on the avian H1 A/widgeon/Wisconsin/505/1979 HA sequence (accession: CY179395). We prune the outgroup sequence and then reconstruct mutations along branches using Treetime. The resulting trees of 901 avian H1NX (https://nextstrain.org/groups/blab/avian/H1) and 1284 avian H3NX strains

17

(https://nextstrain.org/groups/blab/avian/H3) are saved in Auspice format and are viewable at the links provided.

Human and avian genotype analysis

The predominant amino acids observed amongst human H3N2 and H1N1pdm strains at each egg-adaptive site were determined from all non-egg-passaged strains in the phylogenies used throughout this paper. The avian H3NX and H1NX trees described above were used to determine predominant avian genotypes at these positions. All amino acids observed in 10% or more of the strains were recorded.

Avian H1 and H3 phylogenies, for rates of avian HA evolution

Phylogenies were built as described above in "Avian H1 and H3 phylogenies, for human to avian genotype comparison" except that sequences were aligned to an avian HA reference, rather than a human one. For H1, A/duck/Fujian/83/2013 (accession: KP658040) was used as the reference. For H3, A/duck/Jiangsu/JF356/2014 (accession: KP767641) was used as the reference. Full HA-type trees were then divided into separate lineages in order to calculate rates of synonymous and nonsynonymous mutation as well as a rate of adaptation. These trees can be found in Github repo within `nextstrain_builds/avian_separate_lineages/`.

Rates of evolution for avian and human HAs

Rates of synonymous and nonsynonymous mutation were calculated as the slope of a linear regression fitting synonymous or nonsynonymous mutations over time. Specifically, we tabulated the number of synonymous or nonsynonymous differences between each sample and the root of the tree and then plotted this number versus the sample's date. The code to calculate these rates can be found in `figure_panels/Supplement-AvianHArates/calc_avian_dNdt_and_dSdt.ipynb`. Rates of adaptive evolution are calculated using the same code as in Kistler and Bedford, 2023(Kistler and Bedford 2023). The code to calculate rates of adaptation can be found in `figure_panels/Supplement-AvianHArates/calc_avian_ha_dA_rates.ipynb`.

Fixations in human influenza

Using alignments of only human influenza viruses, we calculated mutational frequencies over time with the Augur tool "augur frequencies" (Huddleston et al. 2021). These are saved in the Github repo within `nextstrain_builds/human-influenza-freqs/`. In `figure_panels/Supp-CompareHumanFixationsEggMuts.ipynb` we use these frequencies to find all fixations that occurred during the same time period as the rest of this manuscript. We define a fixation as a mutation that reaches at least 95% frequency within the population.

References

Anon. History of the Influenza Vaccine. *World Health Organization* [Internet]. Available from: https://www.who.int/news-room/spotlight/history-of-vaccination/history-of-influenza-vaccination

Bedford T, Suchard MA, Lemey P, Dudas G, Gregory V, Hay AJ, McCauley JW, Russell CA, Smith DJ, Rambaut A. 2014. Integrating influenza antigenic dynamics with molecular evolution. *Elife* 3:e01914.

Chenavas S, Estrozi LF, Slama-Schwok A, Delmas B, Di Primo C, Baudin F, Li X, Crépin T, Ruigrok RWH. 2013. Monomeric nucleoprotein of influenza A virus. *PLoS Pathog.* 9:e1003275.

Chen G-W, Chang S-C, Mok C-K, Lo Y-L, Kung Y-N, Huang J-H, Shih Y-H, Wang J-Y, Chiang C, Chen C-J, et al. 2006. Genomic signatures of human versus avian influenza A viruses. *Emerg. Infect. Dis.* 12:1353–1360.

Chen Z, Aspelund A, Jin H. 2008. Stabilizing the glycosylation pattern of influenza B hemagglutinin following adaptation to growth in eggs. *Vaccine* 26:361–371.

Chen Z, Zhou H, Jin H. 2010. The impact of key amino acid substitutions in the hemagglutinin of influenza A (H3N2) viruses on vaccine production and antibody response. *Vaccine* 28:4079–4085.

Cros JF, García-Sastre A, Palese P. 2005. An unconventional NLS is critical for the nuclear import of the influenza A virus nucleoprotein and ribonucleoprotein: Role of the unconventional NLS of the influenza A virus NP. *Traffic* 6:205–213.

Dadonaite B, Ahn JJ, Ort JT, Yu J, Furey C, Dosey A, Hannon WW, Vincent Baker AL, Webby RJ, King NP, et al. 2024. Deep mutational scanning of H5 hemagglutinin to inform influenza virus surveillance. *PLoS Biol.* 22:e3002916.

Dawid A, Kiviet DJ, Kogenaru M, de Vos M, Tans SJ. 2010. Multiple peaks and reciprocal sign epistasis in an empirically determined genotype-phenotype landscape. *Chaos* 20:026105.

Dreyfus C, Laursen NS, Kwaks T, Zuijdgeest D, Khayat R, Ekiert DC, Lee JH, Metlagel Z, Bujny MV, Jongeneelen M, et al. 2012. Highly conserved protective epitopes on influenza B viruses. *Science* 337:1343–1348.

Erin Azbazdar M, Dikmenogullari M, Coven FO, Nalbantsoy A, Coven F, Kocer ZA. 2022. Egg Adaptation of Human H1n1 Influenza Virus for Vaccine Production. In: 16th Vaccine Congress. Available from: https://ssrn.com/abstract=4251984

Fisher RA. 1930. The genetical theory of natural selection. Oxford: Clarendon Press

Francis T, Salk JE, Pearson HE, Brown PN. 1945. Protective effect of vaccination against induced influenza a. *J. Clin. Invest.* 24:536–546.

1 Gabriel G, Klingel K, Otte A, Thiele S, Hudjetz B, Arman-Kalcek G, Sauter M, Shmidt T,
2 Rother F, Baumgarte S, et al. 2011. Differential use of importin-α isoforms governs cell
3 tropism and host adaptation of influenza virus. *Nat. Commun.* 2:156.

4 Gambaryan AS, Robertson JS, Matrosovich MN. 1999. Effects of egg-adaptation on the
5 receptor-binding properties of human influenza A and B viruses. *Virology* 258:232–239.

6 Garretson TA, Petrie JG, Martin ET, Monto AS, Hensley SE. 2018. Identification of human
7 vaccinees that possess antibodies targeting the egg-adapted hemagglutinin receptor
8 binding site of an H1N1 influenza vaccine strain. *Vaccine* 36:4095–4101.

9 Hay AJ, McCauley JW. 2018. The WHO global influenza surveillance and response system
10 (GISRS)-A future perspective. *Influenza Other Respi. Viruses* 12:551–557.

11 Huddleston J, Hadfield J, Sibley TR, Lee J, Fay K, Ilcisin M, Harkins E, Bedford T, Neher
12 RA, Hodcroft EB. 2021. Augur: a bioinformatics toolkit for phylogenetic analyses of human
13 pathogens. *J Open Source Softw* [Internet] 6. Available from:
14 http://dx.doi.org/10.21105/joss.02906

15 Jin H, Zhou H, Liu H, Chan W, Adhikary L, Mahmood K, Lee M-S, Kemble G. 2005. Two
16 residues in the hemagglutinin of A/Fujian/411/02-like influenza viruses are responsible for
17 antigenic drift from A/Panama/2007/99. *Virology* 336:113–119.

18 Judge A, Sankaran B, Hu L, Palaniappan M, Birgy A, Prasad BVV, Palzkill T. 2024.
19 Network of epistatic interactions in an enzyme active site revealed by large-scale deep
20 mutational scanning. *Proc. Natl. Acad. Sci. U. S. A.* 121:e2313513121.

21 Kistler KE, Bedford T. 2023. An atlas of continuous adaptive evolution in endemic human
22 viruses. *Cell Host Microbe* 31:1898–1909.e3.

23 Knight ML, Fan H, Bauer DLV, Grimes JM, Fodor E, Keown JR. 2021. Structure of an
24 H3N2 influenza virus nucleoprotein. *Acta Crystallogr. F Struct. Biol. Commun.* 77:208–214.

25 Kukol A, Hughes DJ. 2014. Large-scale analysis of influenza A virus nucleoprotein
26 sequence conservation reveals potential drug-target sites. *Virology* 454-455:40–47.

27 Langat P, Raghwani J, Dudas G, Bowden TA, Edwards S, Gall A, Bedford T, Rambaut A,
28 Daniels RS, Russell CA, et al. 2017. Genome-wide evolutionary dynamics of influenza B
29 viruses on a global scale. *PLoS Pathog.* 13:e1006749.

30 Liang W, Tan TJC, Wang Y, Lv H, Sun Y, Bruzzone R, Mok CKP, Wu NC. 2022. Egg-
31 adaptive mutations of human influenza H3N2 virus are contingent on natural evolution.
32 *PLoS Pathog.* 18:e1010875.

33 Lin YP, Xiong X, Wharton SA, Martin SR, Coombs PJ, Vachieri SG, Christodoulou E,
34 Walker PA, Liu J, Skehel JJ, et al. 2012. Evolution of the receptor binding properties of the
35 influenza A(H3N2) hemagglutinin. *Proc. Natl. Acad. Sci. U. S. A.* 109:21474–21479.

36 Liu F, Gross FL, Joshi S, Gaglani M, Naleway AL, Murthy K, Groom HC, Wesley MG,
37 Edwards LJ, Grant L, et al. 2024. Redirecting antibody responses from egg-adapted
38 epitopes following repeat vaccination with recombinant or cell culture-based versus egg-
39 based influenza vaccines. *Nat. Commun.* 15:254.

Liu F, Tzeng W-P, Horner L, Kamal RP, Tatum HR, Blanchard EG, Xu X, York I, Tumpey TM, Katz JM, et al. 2018. Influence of immune priming and egg adaptation in the vaccine on antibody responses to circulating A(H1N1)pdm09 viruses after influenza vaccination in adults. *J. Infect. Dis.* 218:1571–1581.

Lu B, Zhou H, Chan W, Kemble G, Jin H. 2006. Single amino acid substitutions in the hemagglutinin of influenza A/Singapore/21/04 (H3N2) increase virus growth in embryonated chicken eggs. *Vaccine* 24:6691–6693.

Moutinho AF, Eyre-Walker A, Dutheil JY. 2022. Strong evidence for the adaptive walk model of gene evolution in Drosophila and Arabidopsis. *PLoS Biol.* 20:e3001775.

Ni F, Kondrashkina E, Wang Q. 2013. Structural basis for the divergent evolution of influenza B virus hemagglutinin. *Virology* 446:112–122.

O'Neill RE, Jaskunas R, Blobel G, Palese P, Moroianu J. 1995. Nuclear import of influenza virus RNA can be mediated by viral nucleoprotein and transport factors required for protein import. *J. Biol. Chem.* 270:22701–22704.

Papkou A, Garcia-Pastor L, Escudero JA, Wagner A. 2023. A rugged yet easily navigable fitness landscape. *Science* 382:eadh3860.

Parker L, Wharton SA, Martin SR, Cross K, Lin Y, Liu Y, Feizi T, Daniels RS, McCauley JW. 2016. Effects of egg-adaptation on receptor-binding and antigenic properties of recent influenza A (H3N2) vaccine viruses. *J. Gen. Virol.* 97:1333–1344.

Powell H, Liu H, Pekosz A. 2021. Changes in sialic acid binding associated with egg adaptation decrease live attenuated influenza virus replication in human nasal epithelial cell cultures. *Vaccine* 39:3225–3235.

Raymond DD, Stewart SM, Lee J, Ferdman J, Bajic G, Do KT, Ernandes MJ, Suphaphiphat P, Settembre EC, Dormitzer PR, et al. 2016. Influenza immunization elicits antibodies specific for an egg-adapted vaccine strain. *Nat. Med.* 22:1465–1469.

Robertson JS, Naeve CW, Webster RG, Bootman JS, Newman R, Schild GC. 1985. Alterations in the hemagglutinin associated with adaptation of influenza B virus to growth in eggs. *Virology* 143:166–174.

Rota PA, Wallis TR, Harmon MW, Rota JS, Kendal AP, Nerome K. 1990. Cocirculation of two distinct evolutionary lineages of influenza type B virus since 1983. *Virology* 175:59–68.

Shi Y, Zhang W, Wang F, Qi J, Wu Y, Song H, Gao F, Bi Y, Zhang Y, Fan Z, et al. 2013. Structures and receptor binding of hemagglutinins from human-infecting H7N9 influenza viruses. *Science* 342:243–247.

Skowronski DM, Janjua NZ, De Serres G, Sabaiduc S, Eshaghi A, Dickinson JA, Fonseca K, Winter A-L, Gubbay JB, Krajden M, et al. 2014. Low 2012–13 Influenza Vaccine Effectiveness Associated with Mutation in the Egg-Adapted H3N2 Vaccine Strain Not Antigenic Drift in Circulating Viruses. *PLoS One* 9:e92153.

Smith JM. 1970. Natural selection and the concept of a protein space. *Nature* 225:563–564.

Suptawiwat O, Jeamtua W, Boonarkart C, Kongchanagul A, Puthawathana P, Auewarakul

21

P. 2013. Effects of the Q223R mutation in the hemagglutinin (HA) of egg-adapted pandemic 2009 (H1N1) influenza A virus on virus growth and binding of HA to human- and avian-type cell receptors. *Acta Virol.* 57:333–338.

Suzuki Y, Nei M. 2002. Origin and evolution of influenza virus hemagglutinin genes. *Mol. Biol. Evol.* 19:501–509.

Virk RK, Jayakumar J, Mendenhall IH, Moorthy M, Lam P, Linster M, Lim J, Lin C, Oon LLE, Lee HK, et al. 2020. Divergent evolutionary trajectories of influenza B viruses underlie their contemporaneous epidemic activity. *Proc. Natl. Acad. Sci. U. S. A.* 117:619–628.

Wang Q, Tian X, Chen X, Ma J. 2007. Structural basis for receptor specificity of influenza B virus hemagglutinin. *Proc. Natl. Acad. Sci. U. S. A.* 104:16874–16879.

Weinreich DM, Delaney NF, Depristo MA, Hartl DL. 2006. Darwinian evolution can follow only very few mutational paths to fitter proteins. *Science* 312:111–114.

Widjaja L, Ilyushina N, Webster RG, Webby RJ. 2006. Molecular changes associated with adaptation of human influenza A virus in embryonated chicken eggs. *Virology* 350:137–145.

Wilson JL, Zhou R, Liu H, Rothman R, Fenstermacher KZ, Pekosz A. 2022. Antigenic alteration of 2017-2018 season influenza B vaccine by egg-culture adaption. *Front. Virol.* [Internet] 2. Available from: https://www.frontiersin.org/journals/virology/articles/10.3389/fviro.2022.933440/full

Wu NC, Lv H, Thompson AJ, Wu DC, Ng WWS, Kadam RU, Lin C-W, Nycholat CM, McBride R, Liang W, et al. 2019. Preventing an Antigenically Disruptive Mutation in Egg-Based H3N2 Seasonal Influenza Vaccines by Mutational Incompatibility. *Cell Host Microbe* [Internet]. Available from: http://dx.doi.org/10.1016/j.chom.2019.04.013

Wu NC, Xie J, Zheng T, Nycholat CM, Grande G, Paulson JC, Lerner RA, Wilson IA. 2017. Diversity of functionally permissive sequences in the receptor-binding site of influenza hemagglutinin. *Cell Host Microbe* 21:742–753.e8.

Xu R, McBride R, Nycholat CM, Paulson JC, Wilson IA. 2012. Structural characterization of the hemagglutinin receptor specificity from the 2009 H1N1 influenza pandemic. *J. Virol.* 86:982–990.

Zost SJ, Parkhouse K, Gumina ME, Kim K, Diaz Perez S, Wilson PC, Treanor JJ, Sant AJ, Cobey S, Hensley SE. 2017. Contemporary H3N2 influenza viruses have a glycosylation site that alters binding of antibodies elicited by egg-adapted vaccine strains. *Proceedings of the National Academy of Sciences* 114:201712377.\

22

Figure Legends

Figure 1. Identification of mutations occurring during egg-passaging of human influenza viruses.
A) Phylogeny of 10,415 human influenza A/H3N2 HA sequences (grey), and 1032 egg-passaged strains (purple) sampled between 1995 and 2025. For each year, the proportion of tips that are egg-passaged strains is indicated by the histogram below. B-D) HA phylogenies of egg-passaged strains in the context of non-egg-passaged human influenza virus for A/H1N1pdm (B), B/Vic (C) and B/Yam viruses (D). E) The proportion of egg-passaged strains that were sequenced prior to egg-passaging (pair) is shown for each virus. F) Zoomed view of one clade from the A/H3N2 tree, showing an example of a strain that was sequenced before and after egg-passaging (tip 1), and two strains that were not sequenced prior to egg-passaging where the unpassaged genotype can be inferred from the most closely-related unpassaged strains (tips 2 and 3). The square tip markers indicate a "pair" of sequences of the same strain before and after egg-passaging. Mutations occurring along terminal branches leading to egg-passaged strains are inferred to have occurred during egg-passaging. HA nonsynonymous mutations are labeled along terminal branches.

Figure 2. Mutations occur throughout the influenza genome during egg-passaging but amino acid changes are particularly focused in the HA segment, and inferred adaptive mutations are concentrated within the RBD. A) For each influenza subtype, the proportion of egg-passaged strains that got at least one nonsynonymous (dark), or one synonymous (light) mutation during egg-passaging is shown for the coding region of each segment of the influenza virus. B) The proportion of all egg-passaged strains with an amino acid change is plotted at each residue along the coding region of the segment, for each segment. Y-axis and x-axis scales are shared between plots. C-F) The proportion of all egg-passaged viruses that fixed an amino acid substitution is plotted at each residue along the length of the HA protein for C) A/H3N2, D) A/H1N1pdm, E) B/Vic, and F) B/Yam. The location of the RBD is shaded and the positions of inferred egg-adaptive mutations are colored according to whether they fall within a structural feature of the receptor-binding pocket (130 (influenza A) or 140 (influenza B)-loop = yellow, 150-loop = red, 190-helix = purple, 220-loop = blue) or not (green). Below each plot, the residue number and adaptive amino acid substitutions are listed for each adaptive mutation.

Figure 3. Egg-adaptive mutations change over time as the human influenza virus evolves. The proportion of egg-passaged strains with a mutation at each egg-adaptive residue is calculated in 3-year sliding windows and plotted as a heatmap for A) H3N2, B) H1N1pdm, C) Vic, and D) Yam. For each residue where substitutions to multiple amino acids are observed, the frequency of each of those substitutions is plotted over time.

Figure 4. Egg-adaptive mutations depend on the genotype of the human influenza virus at the same codon. Temporal restriction of adaptive mutations can depend on the human virus' genotype at the same codon position of egg-adaptation via selection against the human genotype (A) or mutational accessibility (B). The location of egg-passaged strains with adaptive mutations (green circles) is shown on the phylogeny on top of the genotype of the circulating human influenza virus (colored branches). Below each phylogeny, a frequency plot uses the same colors to indicate the proportion of human influenza viruses with each genotype over time, and the bar plot indicates proportion of egg-passaged strains with each egg-adaptive mutation, by year.

Figure 5. Egg-adaptive mutations epistatically depend on the genotype of the human influenza virus at nearby residues. The distribution of egg-passaged strains with adaptive mutations (green

23

1   circles) is shown on the phylogeny on top of the genotype of the circulating human influenza virus
2   (colored branches). Frequency plots below show the proportion of human viruses with a given genotype,
3   with the genotypes indicated by the same colors as in the phylogeny. The bar graph overlaid on these
4   frequency plots shows the proportion of egg-passaged strains with the given mutation for each year in the
5   time series. Below, the interacting positions are colored on a structure of hemagglutinin, with the terminus
6   of a sialic acid receptor shown in black. The H3N2 structure is PDB accession 2YP4 (Lin et al. 2012) and
7   the H1N1pdm HA is 3UBE (Xu et al. 2012).
8
9   **Figure 6. Epistatic interactions between egg-adaptive mutations influence their co-occurrence.** A-
10 D) A mutational co-occurrence enrichment score is calculated for each pair of mutations that overlaps
11 temporally as the ratio of observed to expected mutational co-occurrence, specifically by
12 $log2\left(\frac{freqA+B}{freqA * freqB}\right)$ where A and B are the two mutations. Mutations that co-occur more often than
13 expected based on their individual frequencies will have higher (redder) values, and mutations that co-
14 occur less frequently have lower (bluer) values. Mutations that overlap temporally but never co-occur
15 together are shown in dark blue because $log2$ of 0 is undefined. E) The total number of egg-adaptive HA
16 mutations per strain is plotted by influenza subtype. Only strains that get at least one adaptive mutation
17 during egg-passaging are plotted.
18
19 **Figure 7. A given hemagglutinin sequence has access to multiple possible egg-adaptive**
20 **trajectories.** A) Four representative sets of egg-passaged sequences derived from identical unpassaged
21 HA1 sequences are shown for each virus. The "adaptive haplotypes" observed within a set are
22 represented by a string of boxes that are filled in if there was an adaptive mutation at that position. For
23 each subtype, a key denoting which column of boxes corresponds to which position is shown at the top.
24 The number of egg-passaged strains in the set with that "adaptive haplotype" is written to the left. All
25 other sets can be seen in Supplement Figures 4-7. B) The number of adaptive sites mutated amongst
26 each set is plotted over time, with the circle size indicating how many egg-passaged strains are in the set.
27 Each set is plotted at the mean date of all strains within that set. The dashed line indicates the total
28 number of adaptive positions observed throughout all egg-passaged sequences over time (see
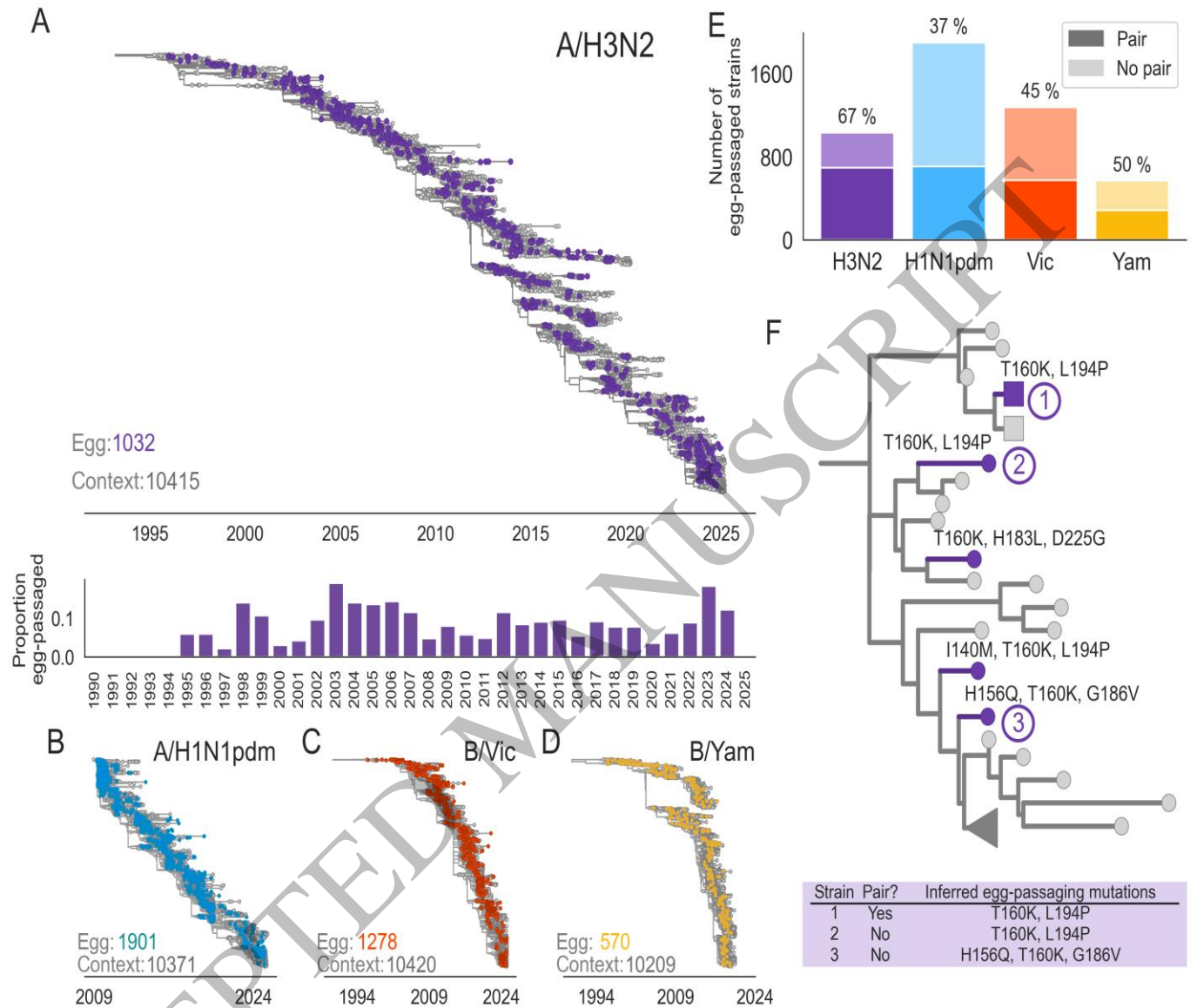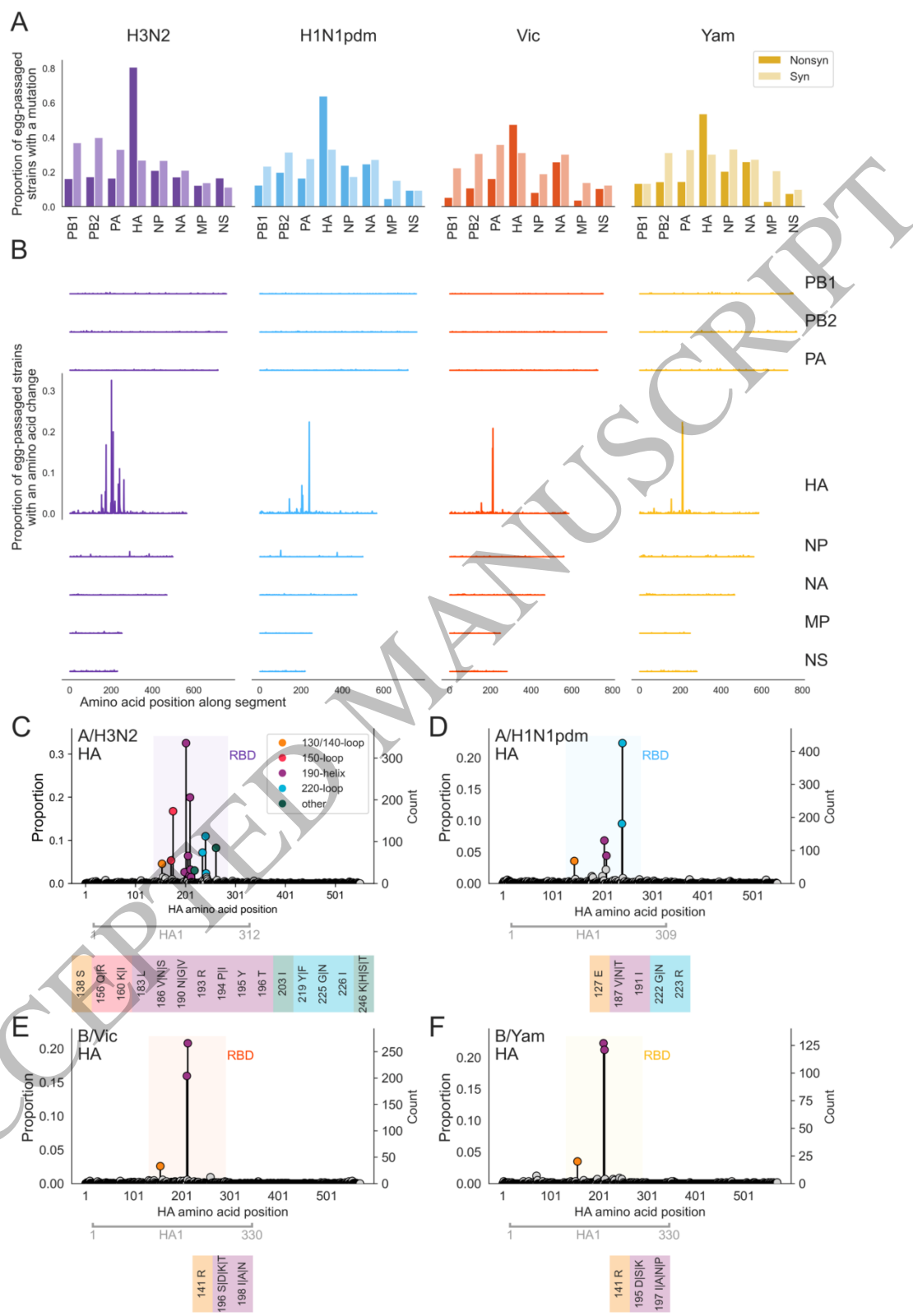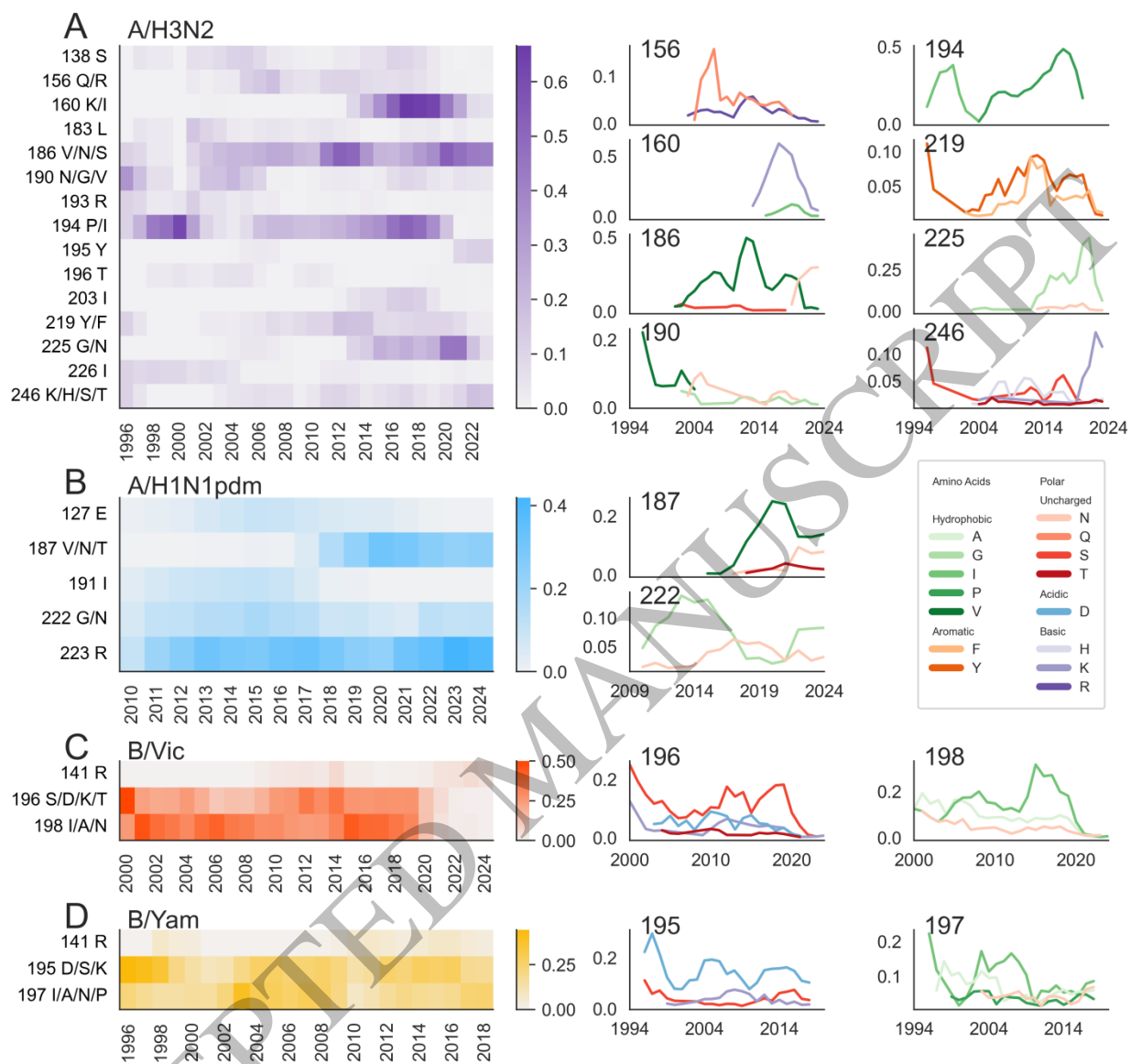29 Supplemental Figure 10).

24

Figure 1
299x208 mm (x DPI)

1

2 **Figure 2**

3 **358x559 mm (x DPI)**

Figure 3
228x214 mm (x DPI)
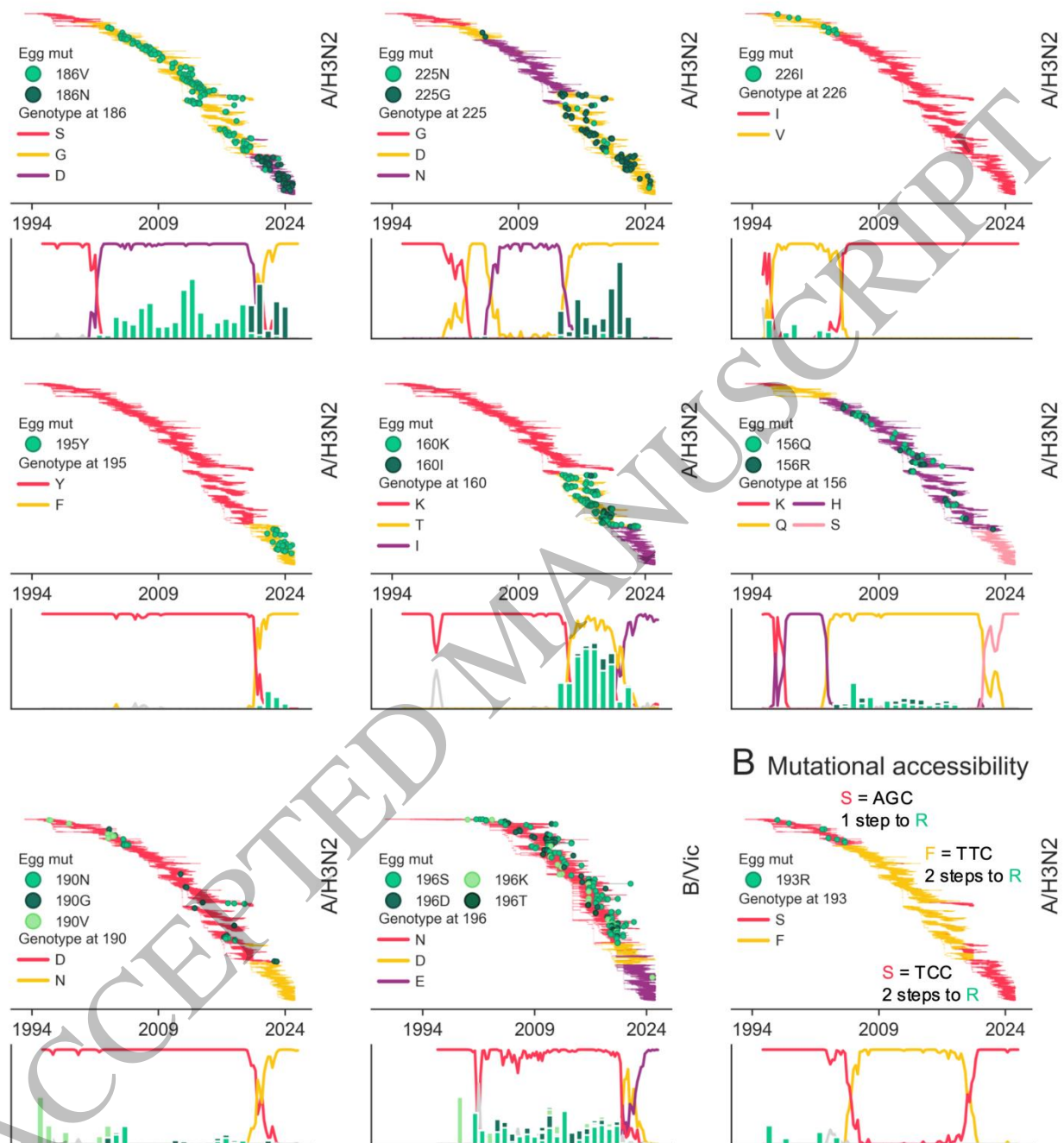
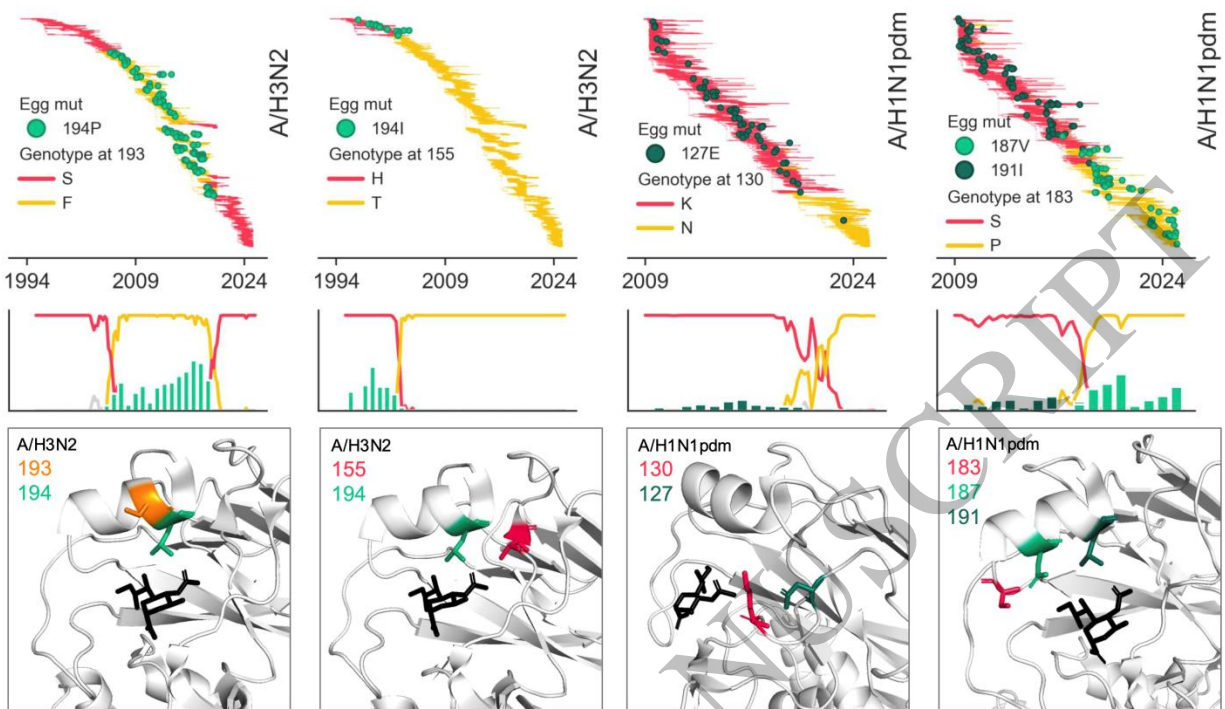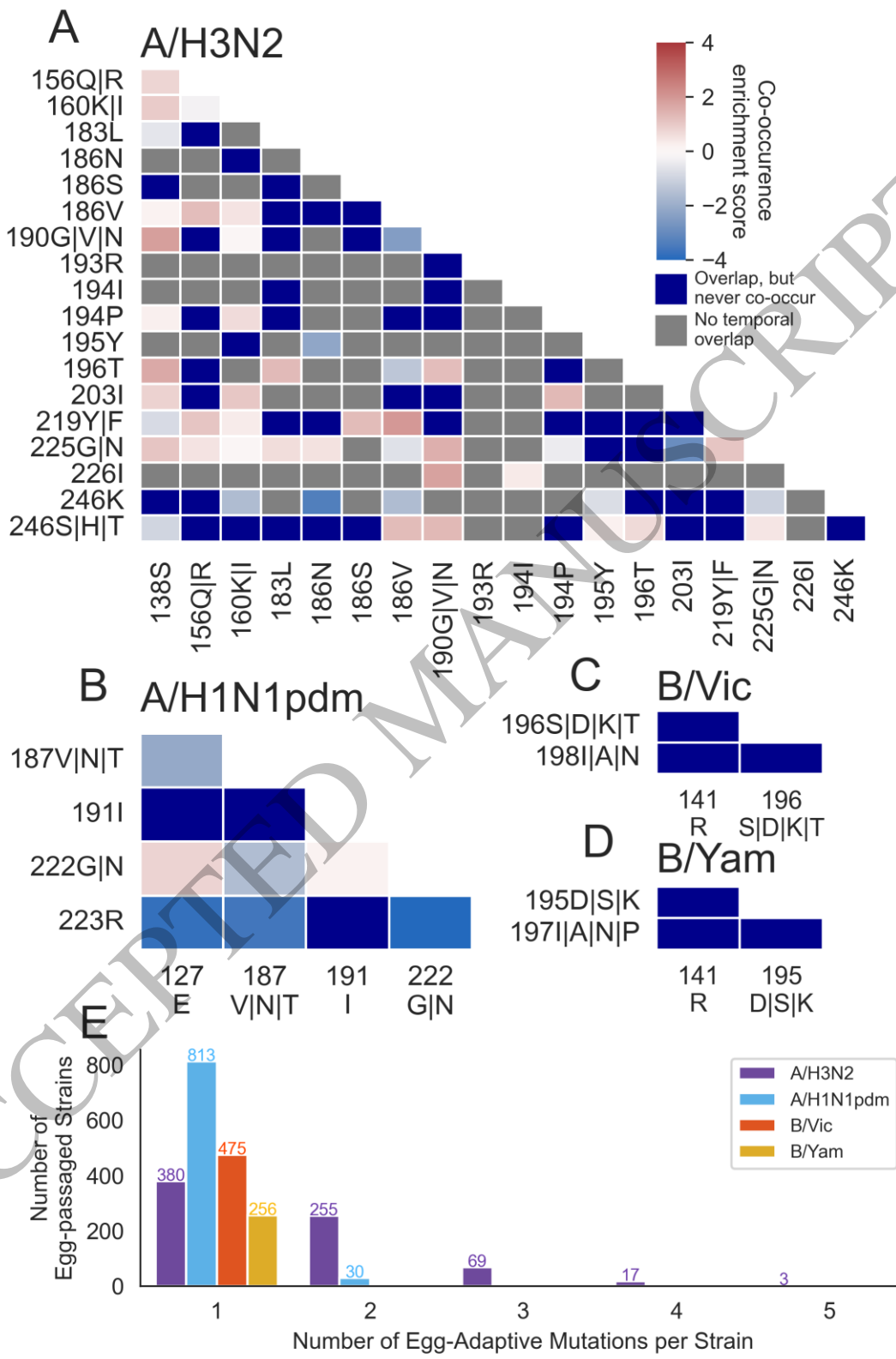**Figure 4**
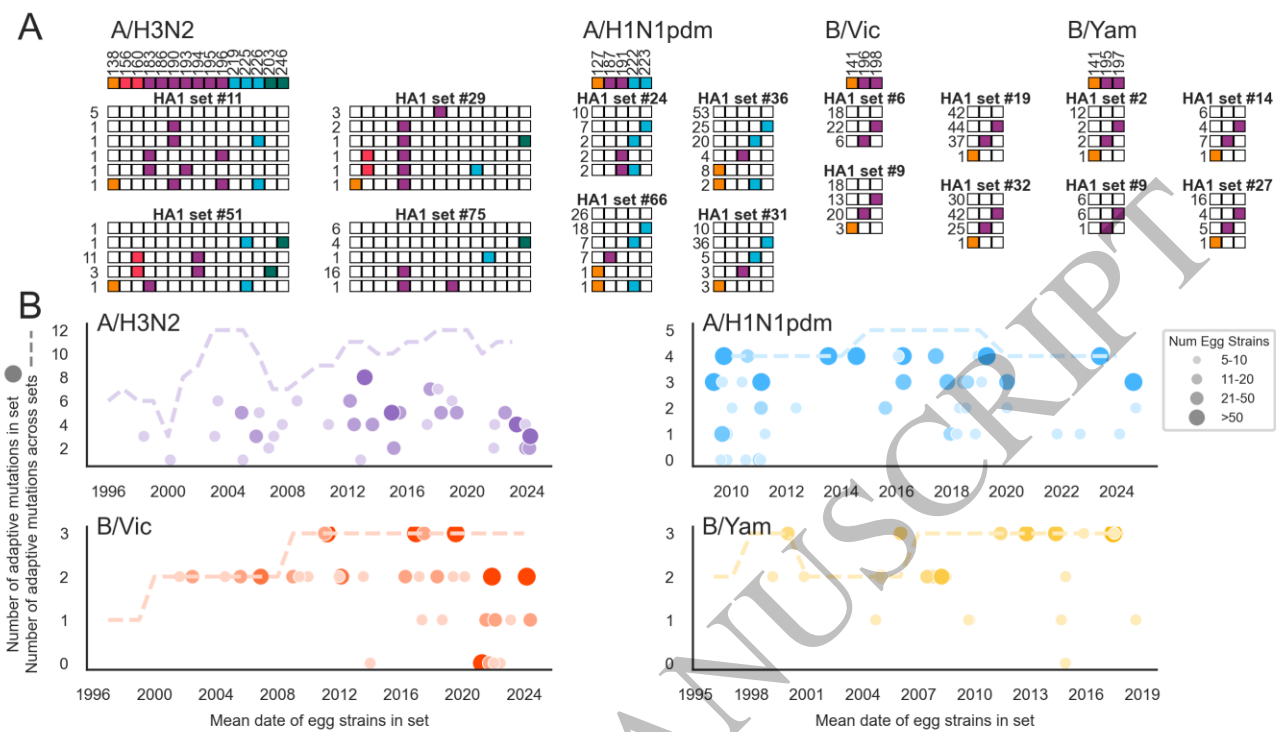**489x559 mm (x DPI)**

Figure 5
559x324 mm (x DPI)

Figure 6
144x212 mm (x DPI)

Figure 7
173x100 mm (x DPI)